Determination of the temporal structure of femtosecond laser pulses by means of laser-induced air plasma*

Zhang Nan(张 楠), Bao Wen-Xia(包文霞), Yang Jing-Hui(杨景辉), and Zhu Xiao-Nong(朱晓农)†

Institute of Modern Optics, Nankai University, Tianjin 300071, *China*
Key Laboratory of Optical Information Science and Technology of Ministry of Education, Nankai University, Tianjin 300071, *China*

(Received 22 August 2012; revised manuscript received 17 October 2012)

A new approach is presented to reveal the temporal structure of femtosecond laser pulses by recording the corresponding time-resolved shadowgraphs of the laser-induced air plasma. It is shown that the temporal structures of femtosecond laser pulses, normally not observable by the ordinary intensity autocorrelator, can be detected through intuitively analyzing the ultrafast evolution process of the air plasma induced by the femtosecond laser pulses under examination. With this method, existence of pre- and post-pulses has been clearly unveiled within the time window of ±150 fs in reference with the main 50-fs laser pulses output from a commercial 1-kHz femtosecond laser amplifier. The unique advantage of the proposed method is that it can directly provide valuable information about the pulse temporal structures' effect on the laser-induced ionization or material ablation.

Keywords: pulse temporal structure, femtosecond laser pulse, air plasma, pump–probe technique

PACS: 42.65.Re, 32.80.–t, 52.50.Jm **DOI:** 10.1088/1674-1056/22/5/054209

1. Introduction

The temporal profile of ultrashort laser pulses is one of the most important factors in the studies of various ultrashort laser-material interactions such as laser-induced target ionization/ablation,[1–3] high-order harmonic generation,[4] optical trapping,[5] etc. Therefore, a number of pulse measurement techniques, such as the third-order autocorrelator,[6] frequency resolved optical gating (FROG),[7] and spectral phase interferometry for direct electric-field reconstruction (SPIDER),[8] have been developed to accurately determine the temporal intensity distribution of an ultrashort laser pulse.

In this paper, a relatively simple and intuitive method is presented for investigating the ultrashort laser pulse structure in the time domain. The proposed method is especially suitable for the pump–probe related experiments. This is because to investigate the pulse temporal structure with this method, the time-resolved shadowgraphs of the air plasma induced by the laser pulses under examination need to be recorded by the pump–probe apparatus. Using this method, pulse structures closely adjacent to the main pulse can be conveniently revealed by analyzing the evolution of the air plasma. Since the method utilizes the interaction between the laser pulses under investigation and the ambient air (or other materials) to unveil the pulse temporal shape, it is especially useful for providing the information about the effect of the pre- or post-pulses on the laser-induced ionization or ablation, which cannot be readily obtained using other measurement methods, such as the third-order autocorrelator, FROG, and SPIDER.

2. Experimental setup

Figure 1(a) shows the experimental setup for investigating the pulse temporal structure of femtosecond laser pulses. A commercial Ti:sapphire femtosecond laser amplifier system (HP-Spitfire, Spectra-Physics Inc.) is employed, which can generate 1-kHz femtosecond laser pulses with a central wavelength of 800 nm and a pulse energy up to 2 mJ. The duration of the output laser pulse is monitored by a single-shot second-order autocorrelator (SSA, Positive Light Inc.). A typical second-order intensity autocorrelation curve of the shortest laser pulses that can be generated by the amplifier is shown in Fig. 1(b). It is deduced that the full-width at half maximum (FWHM) is around 50 fs under the assumption that the laser pulse has a temporal profile of Gaussian shape. The output laser beam from the amplifier also has an approximate Gaussian cross-sectional intensity distribution. It is split into two beams which are respectively used as the pump beam to ionize the ambient air and the probe beam to record the time-resolved shadowgraphs of the ultrafast dynamic process of air plasma.

As shown in Fig. 1(a), a 10× objective (NA = 0.25) is used to focus the pump pulses (i.e., the laser pulses under test). The probe beam is frequency doubled with a 2-mm-thick BBO crystal with type-I phase matching. A short wavelength pass filter (SWPF) is inserted behind the BBO crystal to block the 800-nm fundamental light, and thus only the 400-nm frequency-doubled light passes through the air breakdown region. The time delay between the pump and probe pulses, i.e., the time interval between the time to record the shadowgraph

*Project supported by the National Natural Science Foundation of China (Grant Nos. 11004111 and 61137001), the Natural Science Foundation of Tianjin City, China (Grant No. 10JCZDGX35100), the Specialized Research Fund for the Doctoral Program of Higher Education of China (Grant No. 20100031120034), and the Fundamental Research Funds for the Central Universities of China.

†Corresponding author. E-mail: xnzhu1@nankai.edu.cn

© 2013 Chinese Physical Society and IOP Publishing Ltd

and the time that the ambient air is just ionized, can be conveniently adjusted with the optical delay line. The optical delay line has a spatial resolution of 5 μm, resulting in a time resolution of ∼ 33 fs. The time-resolved shadowgraphs of air plasma are recorded with a 4× objective (NA = 0.1) and a CCD camera (LU135M, Lumenera Inc., sensor size: 6.47×4.84 mm^2). A 400-nm interference filter (IF) with a bandwidth of 10 nm (FWHM) is placed before the CCD camera to block the air plasma's visible emission from entering the CCD camera.

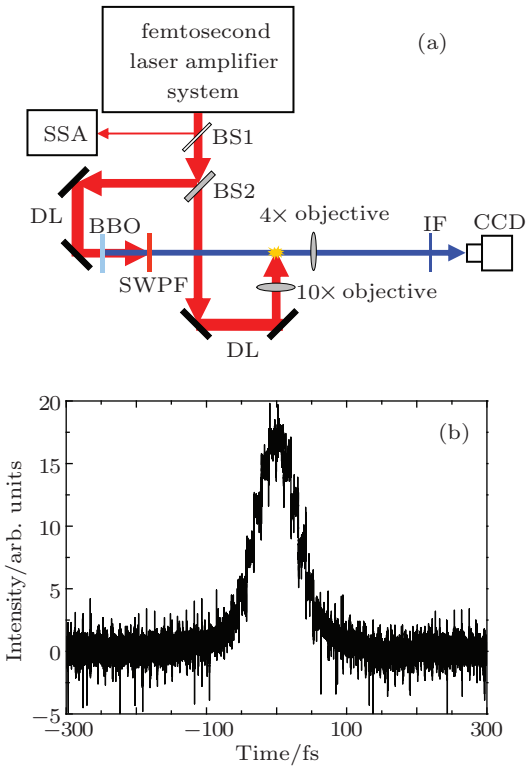


Fig. 1. (color online) (a) Experimental setup for investigating the temporal structure of femtosecond laser pulses by the pump–probe technique. SSA: single-shot autocorrelator; BS: beam splitter; DL: delay line; SWPF: short wavelength pass filter; IF: interference filter. (b) A typical autocorrelation curve of 50-fs laser pulses emitting from the amplifier measured by the SSA.

During the experiment, the pulse repetition rate of the laser system is reduced from 1 kHz to 15 Hz so that it can match the frame rate of the CCD camera. In this way, each shadowgraph is guaranteed to be recorded by a single probe pulse at a particular time delay, presenting a specific transient state of the micro air plasma induced by a single pump pulse. It is noted that the measurement apparatus in Fig. 1(a) can be actually further simplified by replacing the BBO crystal, SWPF, and IF with some neutral density filters placed before the CCD camera, if the scattered light of the pump pulse and the plasma emission from the ionization region are not very strong.

3. Results and discussion

Figure 2 presents the recorded time-resolved shadowgraphs of air plasma induced by the femtosecond laser pulses under examination. For Figs. 2(b)–2(e), the energy of the pump laser pulse after the focusing objective is 135 μJ; and the pump laser pulse has the shortest pulse width that the laser system can achieve, which is ∼ 50 fs (FWHM). As the pump pulse passes through several optical components including a 10× objective before it arrives at the actual focal point, extra dispersion is exerted on the pulses. Such additional dispersion must be compensated to make the pulse width maintain 50 fs at the focus. This is achieved by slightly adjusting the effective grating pair separation of the pulse compressor inside the femtosecond laser amplifier system. During the adjustment, the optimal dispersion compensation for the pump laser pulse at the air breakdown region is achieved when the highest brightness of the air plasma emission occurs. The brightness of air plasma emission can be easily monitored by using the optical setup shown in Fig. 1(a), but blocking the probe beam and removing the interference filter.

During the experiments, before a shadowgraph of air plasma is taken, a background shadowgraph is always recorded with the pump laser beam blocked. Such a background picture is shown in Fig. 2(a). Also, as indicated by the solid arrow in Fig. 2(a), the focused pump laser beam propagates from the right to the left for all pictures in Fig. 2. The area enclosed by the two hyperbolic lines and two vertical lines in Fig. 2(a) approximately represents the air breakdown region induced by the focused femtosecond laser pulses under test, which is determined primarily with the help of the recorded shadowgraph given by Fig. 2(e). Note that after the time delay of 0.6 ps (see Fig. 2(e)), the shape and size of the plasma channel remain nearly steady until subsequent plasma expanding process occurs. This is the reason why Fig. 2(e) is used to determine the air breakdown region in Fig. 2(a). By comparing Fig. 2(b) with Fig. 2(a), we can see that a short plasma channel just appears on the right side of Fig. 2(b). This can be observed more clearly from the pseudo-color picture in the upper right corner of Fig. 2(b). For all the pseudo-colored insert pictures in Fig. 2, they are obtained after the corresponding background picture is subtracted. In the pseudo-color picture (i.e., Fig. 2(b)), the short plasma channel appears as several nearly-parallel horizontal lines, which may be the filament bunch generated under the relatively tight focusing condition.[9] The filament bunch can be seen more obviously in Figs. 2(c)–2(g) for larger time delays. In principle, the absolute zero time delay in pump–probe experiments should be defined as the time when the peak of the pump pulse just overlaps with the peak of the probe pulse, but a consistent relative zero time delay is needed in our case. From the air breakdown region shown in Fig. 2(a), it can be seen that the short plasma channel in Fig. 2(b) occurs at the outskirts of the air breakdown region, which means that it is generated by the part of the pump pulse associated with the maximal light intensity. Therefore, the zero time in Fig. 2(b)

corresponds to the time when the pump pulse's peak just arrives at the location of the short plasma channel in Fig. 2(b). Such a definition is convenient for us to analyze the air plasma channel's evolution in relation with the pump pulse's propagating process through the focal region.

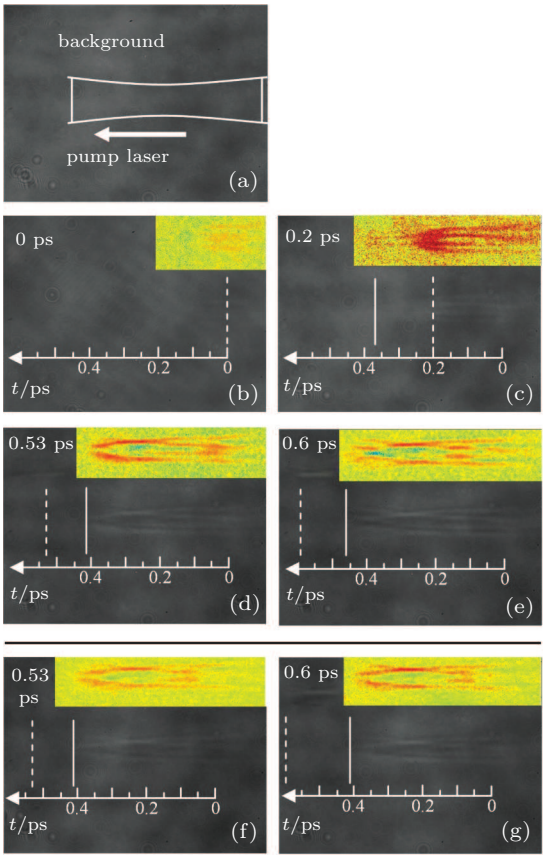


Fig. 2. (color online) Time-resolved shadowgraphs of air plasma generated by the femtosecond laser pulses under test at indicated time delays. (a) Background shadowgraph recorded when the pump pulse is blocked; (b)–(g) the corresponding pseudo-color picture of the recorded air plasma is added in the upper right corner of each picture. The size of the pseudo-color picture is however different from each other because it is obtained by clipping from the original shadowgraph. The time axis that points to the left presents the time needed for light to arrive at the specific position. The vertical dashed/solid lines mark the position of the pump pulse peak/the front of the corresponding air plasma channel, respectively. (f), (g) In reference to panels (d) and (e), the compressor of the femtosecond laser amplifier and the corresponding pulse dumping time are carefully adjusted and the pump pulse energy after the 10× objective becomes 114 μJ, but the pump pulse duration keeps almost unchanged. Frame size: 230×172 μm^2.

It is estimated that in our experiments, the air plasma is induced by the femtosecond pump pulse with an average field strength of ∼ 43.2 V/Å, and thus the main ionization mechanism is the tunnelling ionization that happens within few femtoseconds after the laser irradiation.[10,11] Therefore, it is appropriate to take the center of the plasma channel in Fig. 2(b) as the peak position of the pump laser pulse at zero time delay. This position is marked by the vertical dashed line. It can be inferred that the error of the pump pulse peak position will be determined by the half length of the plasma channel (see Fig. 2(b)). Although this could correspond to a maximum error of ∼ 60 fs in Fig. 2(b), it can be decreased by recording an even shorter plasma channel. Hence, this will not be an obstacle for the presented method of investigating the temporal shape. In addition, because our main interest is to investigate the position and intensity of the pre- and post-pulses, rather than the pulse duration of the main pulse, the error is acceptable and will not affect the correct determination of the presence of the pre- and post-pulses. The error occurring in the determination of the pump pulse peak, not the duration of the probe pulse, determines the time resolution of investigating the pulse structure presented in Figs. 1 and 2.

In Fig. 2(c), for the time delay of 0.2 ps, the probe pulse falls behind the pump pulse by 0.2 ps. The peak of the pump pulse (dashed line) propagates from the right to the left by a distance of 60 μm, whereas the front of the laser-induced air plasma channel appears to reach the location indicated by the solid line. This is clearly confirmed in the pseudo-color picture (i.e., upper right corner of Fig. 2(c)). As it is impossible for the plasma to move faster than light, Fig. 2(c) only demonstrates that a pre-pulse or pulse leading pedestal exists for ∼ 150 fs before the main pulse peak and it is intense enough to ionize the ambient air before the main pulse arrives. It is known that the high intensity of the laser pulse in the focal region may induce strong nonlinear optical effects which can result in the pulse splitting in the time domain.[12] However, in our case, as it is not likely that there is strong pre-formed plasma when the pre-pulse or pulse leading part propagates through, the pulse leading part observed through Fig. 2(c) is considered to be the intrinsic structure of the pump pulse and not originated from the pulse temporal modulation in the focal region.

When time elapses to 0.53 ps, it can be seen from Fig. 2(d) that the peak of the pump pulse (dashed line) just leaving the focal region, becomes over 0.1 ps ahead of the front of the laser-induced air plasma channel (solid line). The plasma channel in Fig. 2(d) looks more clearly than the one in Fig. 2(c) since the pump pulse peak with maximal light intensity has propagated through the whole plasma channel at this time delay. The fact that the peak of the pump pulse does not ionize the ambient air located between the solid and the dashed lines in Fig. 2(d) manifests strong defocusing of the pump laser after propagating through the focal region. However, in Fig. 2(e) of 0.6 ps time delay the front of the laser-induced air plasma channel appears to move forward again. As in this case, the front of the air plasma channel moves forward approximately 15 μm during the time interval of 70 fs, namely with a moving speed of over 2×10^8 m/s. Apparently, the front movement of the plasma channel at this time delay cannot be attributed to the actual evolution of the same air plasma because such an expanding speed would be too high. Therefore, the only possible reason for such a fast movement of the plasma channel could be that a post-pulse after the

main pulse peak arrives and further ionizes the ambient air. The pre-formed air plasma channel induced by the main pulse makes the post-pulse defocus due to its less-than-one refractive index,[13] so the effective focal length for the post-pulse is longer than that for the main pulse, which enables the relatively low-intensity post-pulse to ionize the air near the left side of the solid line in Fig. 2(d), i.e., the air that the main pulse cannot ionize. In Fig. 2(e), since the pump pulse peak is $\sim$ 150 fs ahead of the plasma channel front (see the time axis in Fig. 2(e)), it is estimated that the post-pulse is located at $\sim$ 150 fs after the main pulse peak.

It is known that the temperature drift and high voltage ringing of the Pockel cell employed inside the regenerative amplifier, as well as the parameter settings of the pulse compressor, can all affect the temporal profile of the output laser pulse of the femtosecond laser amplifier system. In our experiment, by carefully adjusting the dumping time and the compressor of the femtosecond laser amplifier system, the post-pulse shown in Fig. 2(e) can be eliminated, or more strictly speaking, the post-pulse's intensity can be brought down below the air ionization threshold. In this case, the energy of the pump pulse arriving at the air ionization region is 114 μJ. Both the pump pulse duration and its normalized autocorrelation curve measured by the SSA keep almost unchanged after these adjustments. The time-resolved shadowgraphs of air plasma induced by the pump pulse without post-pulse are presented in Figs. 2(f) and 2(g). It is noted that the zero point of the time axis at the bottom of Figs. 2(f) and 2(g) moves to the left slightly compared with those in Figs. 2(b)–2(e) due to the slight displacement of the imaging CCD between different groups of experimental trials. From these two pictures, it is observed that the front of the laser-induced air plasma channel does not move forward at 0.6 ps time delay, showing that post-pulses which can ionize the ambient air does not exist. It is considered that as the post-pulse can be eliminated by adjusting the amplifier system, it is unlikely to be originated from the nonlinear optical effects in the focal region, and thus it may be still representative of the actual pulse structure of the pump pulse. The information about the temporal structure of the amplified femtosecond laser pulses obtained from the analyses of the evolution of the laser-induced air plasma cannot be acquired from the autocorrelation curve, such as the one shown in Fig. 1(b).

4. Conclusions

In this paper, a new method for qualitatively investigating the temporal structure of relatively intense ultrashort laser pulses is demonstrated. By recording the time-resolved shadowgraphs of air plasma induced by the femtosecond laser pulses under examination, the effect of the temporal structure of femtosecond laser pulses can be intuitively observed. The existence of both pre- and post-pulses adjacent to the main pulse peak may be verified as long as their intensities are above the air ionization threshold. It is expected that by using other transparent materials, such as inert gases, water, or silica glass, the pulse structure with much lower light intensity can be also observed by this method. As the method described above essentially employs the laser-material interaction to investigate the pulse temporal shape, it may directly provide valuable information for analyzing the effect of the pulse temporal shape on the dynamic processes involved in and the final results of ultrashort laser ionization/ablation.

References

[1] Castro A, Rasanen E, Rubio A and Gross E K U 2009 *Europhys. Lett.* **87** 53001
[2] Bourquard F, Colombier J P, Guillermin M, Loir A S, Donnet C, Stoian R and Garrelie F 2012 *Appl. Surf. Sci.* **258** 9374
[3] Wollenhaupt M, Englert L, Horn A and Baumert T 2010 *Proc. SPIE* **7600** 76000X
[4] Boyko O, Valentin C, Mercier B, Coquelet Ch, Pascal V, Papalazarou E, Rey G and Balcou P 2007 *Phys. Rev. A* **76** 063811
[5] Shane J C, Mazilu M, Lee W M and Dholakia K 2010 *Opt. Express* **18** 7554
[6] Collier J, Hernandez-Gomez C, Allott R, Danson C and Hall A 2001 *Laser Part. Beams* **19** 231
[7] Kane D J and Trebino R 1993 *Opt. Lett.* **18** 823
[8] Chai L, He T, Gao F, Wang Q, Xing Q and Zhang Z 2004 *Chin. Phys.* **13** 1487
[9] Liu X L, Lu X, Liu X, Xi T T, Liu F, Ma J L and Zhang J 2010 *Opt. Express* **18** 26007
[10] Shafir D, Soifer H, Bruner B D, Dagan M, Mairesse Y, Patchkovskii S, Ivanov M Y, Smirnova O and Dudovich N 2012 *Nature* **485** 343
[11] Keldysh L V 1965 *Sov. Phys. JETP* **20** 1307
[12] Wang Z, Zhng C, Liu J and Xu Z 2012 *Opt. Express* **20** 9558
[13] Guo S 1997 *Electrodynamics* (Beijing: High Education Press) pp. 178–179 (in Chinese)